Glycoconj J (2008) 25:313–321
DOI 10.1007/s10719-007-9076-6

SPR and ITC determination of the kinetics and the thermodynamics of bivalent *versus* monovalent sugar ligand–lectin interactions

Bandaru Narasimha Murthy · Sharmistha Sinha · Avadhesha Surolia · Shantinath S. Indi · Narayanaswamy Jayaraman

Received: 24 August 2007 / Revised: 21 September 2007 / Accepted: 26 September 2007 / Published online: 23 October 2007

Abstract A kinetic study of the interaction of bivalent and monovalent sugar ligands with a lectin was undertaken with the aid of surface plasmon resonance (SPR) method. The study involved a series of bivalent α-D-mannopyranoside containing sugar ligands, with systematic variation in the distance between the sugar ligands. The detailed kinetic studies showed that bivalent ligands underwent a faster association (k_{on}) and a slower dissociation (k_{off}) of the ligand–lectin complexes, in comparison to the monovalent ligand–lectin complexes. The kinetic constants were complemented further by assessing the thermodynamic parameters with the aid of isothermal titration calorimetry (ITC). The initiation of cross-linking of ligand–lectin interactions emerge from the early stages of the complexation. The dynamic light scattering (DLS) and the transmission electron microscopy (TEM) techniques allowed judging the sizes and morphologies of the complex in the solution and solid states, respectively.

Keywords Lectins · Surface plasmon resonance · Isothermal titration calorimetry · Sugar ligands · Electron microscopy · Dynamic light scattering

B. N. Murthy · N. Jayaraman (✉)
Department of Organic Chemistry, Indian Institute of Science,
Bangalore 560 012, India
e-mail: jayaraman@orgchem.iisc.ernet.in

S. Sinha · A. Surolia (✉)
National Institute of Immunology,
New Delhi 110 067, India
e-mail: surolia@nii.res.in

S. S. Indi
Department of Microbiology and Cell Biology,
Indian Institute of Science,
Bangalore 560 012, India

Abbreviations

ITC	Isothermal titration calorimetry
SPR	Surface plasmon resonance
CMC	Critical micellar concentration
DLS	Dynamic light scattering
TEM	Transmission electron microscopy

Introduction

Presence of manifold sugar ligands within a molecular scaffold is now established to be beneficial to overcome the weak binding affinities of sugar ligands with carbohydrate binding proteins, namely, lectins [1–5]. The favourable enthalpy changes generally result in a large increase in binding affinities between the multivalent sugar ligands and the lectins [6, 7]. The lectin oligomers often undergo formation of intermolecular cross-linked complexes upon binding with multivalent sugar ligands. A large number of studies explored a variety of synthetic and semi-synthetic multivalent sugar ligands and their abilities to significantly enhance the lectin binding affinities [8–17]. It is seen, however, that the studies of the kinetics of the ligand–lectin interactions are much less known [18, 19]. In our continuing studies on multivalent interactions [20–23], we undertook a detailed study of the kinetics of the bivalent *vs* monovalent sugar ligands during the lectin binding, by employing the SPR technique. The results were correlated with thermodynamic parameters, secured from the ITC measurements. In addition, an effort to identify the hydrodynamic diameters and the morphologies of the ligand–lectin complexes was also undertaken by involving DLS and TEM. The results of this combined study are presented herein.

Materials and methods

General methods

Solvents were dried and distilled according to literature procedures. All chemicals were purchased from commercial sources and were used without further purifications. Analytical TLC was performed on commercial plates coated with silica gel GF_{254} (0.25 mm). Silica gel (100–200 mesh) was used for column chromatography. Micro-analyses were performed on an automated C, H and N analyzer. High-resolution mass spectra were obtained from Q-TOF instrument by electrospray ionization (ESI). ^{1}H and ^{13}C NMR spectral analyses were performed on a spectrometer operating at 300 and 75 MHz, respectively, and residual solvent signal was used as the internal standard. Lectin concanavalin A (Con A) and wheat germ agglutinin (WGA) (salt free, lyophilized powder) were purchased from Sigma. Aqueous solutions were prepared from double distilled water purified through a Milli Q to 18.2 MΩ resistance. All ligand–lectin binding experiments were performed in 10 mM HEPES buffer containing 150 mM NaCl, 1 mM $CaCl_2$ and 1 mM $MnCl_2$. Buffer solution was filtered (0.2 μm) and thoroughly degassed.

General procedure for synthesis of sugar ligands *1* to *8*

To a suspension of appropriate 2-*O*-alkyl-glycerol derivative [24], $Hg(CN)_2$, $HgBr_2$ and molecular sieves (4 Å) in CH_2Cl_2, a solution of 2,3,4,6-tetra-*O*-benzoyl-α-D-mannopyaranosyl bromide [25] in CH_2Cl_2 was added under stirring at room temperature and under argon atmosphere. The mixture was stirred for 36 h, then it was filtered through celite, washed with CH_2Cl_2 and the organic layer was washed with aq. $Na_2S_2O_3$ (10%), aq. $NaHCO_3$ (5%) and H_2O. The CH_2Cl_2 layer was dried (Na_2SO_4), filtered, concentrated *in vacuo* and the residue was purified (SiO_2, petroleum ether/EtOAc) to afford the *O*-benzoyl-protected sugar ligands. A suspension of the protected sugar ligand in MeOH was admixed with NaOMe/MeOH (0.5 M, 0.5 ml) and left stirring for 12 h, then neutralized with Amberlite IR-120 resin (H^+ form), filtered and the filtrate concentrated *in vacuo*. The resulting gummy syrup was triturated with Et_2O and lyophilized to afford the sugar ligands, as white foamy powders.

2-Dodecyloxy-3-O-(α-D-mannopyranosyl)-propane-1-ol (1)

Yield: 38%, R_f=0.35 (MeOH/$CHCl_3$=1:6), $[\alpha]_D^{24} = +39°$ (c=1.0, MeOH). ^{1}H NMR Acetone-d_6, 300 MHz): δ4.77 (d, 1 H, J=3.6 Hz), 3.99 (br s, 1 H), 3.84–3.41 (band, 12 H), 1.53 (m, 2 H), 1.29 (br s, 18 H), 0.88 (t, 3 H, J=6.9 Hz). ^{13}C NMR (Acetone-d_6, 75.5 MHz): δ101.4, 80.3, 80.2, 73.9, 72.6, 71.7, 68.9, 67.7, 63.0, 62.5, 32.6–23.7, 14.30. ESI-MS *m/z*: calcd. for $C_{21}H_{42}O_8Na$: 445.2777; found: 445.2791 (M+Na). Anal. calcd. for $C_{21}H_{42}O_8$: C 59.69, H 10.02; found: C 59.89, H: 9.79.

5-Dodecyloxy-9-O-(α-D-mannopyranosyl)-3, 7-dioxaononane-1-ol (2)

Yield: 40%, R_f=0.45 (MeOH/$CHCl_3$=1:4), $[\alpha]_D^{24} = +26°$ (c=1.0, MeOH). ^{1}H NMR (Acetone-d_6, 300 MHz): δ4.81 (d, 1 H, J=1.5 Hz), 4.02 (m, 1 H), 3.88 (d, 1 H, J=3.9 Hz), 3.80–3.45 (band, 19 H), 1.50 (m, 2 H), 1.29 (br s, 18 H), 0.88 (t, 3 H, J=6.9 Hz). ^{13}C NMR (Acetone-d_6, 75 MHz): δ101.1, 78.8, 77.3, 73.9, 73.8, 72.6, 71.8, 71.7, 71.1, 70.8, 69.1, 67.1, 63.1, 61.9, 32.6–23.3, 14.3. ESI-MS *m/z*: calcd. for $C_{25}H_{50}O_{10}Na$: 533.3302; found: 533.3300 (M+Na). Anal. calcd. for $C_{25}H_{50}O_{10}$:C 58.08, H 9.87; found: C 58.34, H 9.90.

8-Dodecyloxy-15-O-(α-D-mannopyranosyl)-3,6, 10, 13-tetraoxaopentadecan-1-ol (3)

Yield: 43%, R_f=0.4 (MeOH/$CHCl_3$=1:4), $[\alpha]_D^{24} = +32°$ (c=1.0, MeOH). ^{1}H NMR (Acetone-d_6, 300 MHz): δ4.79 (br s, 1 H), 4.04 (m, 1 H), 3.84–3.75 (band, 4 H), 3.66–3.45 (band, 24 H), 1.40 (m, 2 H), 1.27 (br s, 18 H), 0.88 (t, 3 H, J=6.9 Hz). ^{13}C NMR (Acetone-d_6, 75.5 MHz): δ101.1, 78.8, 73.9, 73.5, 72.5, 71.9–70.7, 68.9, 67.2, 63.0, 61.9, 32.6–23.7, 14.3. ESI-MS *m/z*: calcd. for $C_{29}H_{58}O_{12}Na$: 621.3826; found: 621.3846 (M+Na). Anal. calcd. for $C_{29}H_{58}O_{12}$: C 58.17, H 9.76; found: C 57.93, H 9.77.

2-Methoxy-3-O-(α-D-mannopyranosyl)-propane-1-ol (4)

Yield: 32%, R_f=0.1 (MeOH/$CHCl_3$=1:4), $[\alpha]_D^{24} = +48°$ (c=1.0, MeOH). ^{1}H NMR (D_2O, 300 MHz): δ4.70 (br s, 1 H), 3.79–3.54 (band, 11 H), 3.26 (s, 3 H). ^{13}C NMR (D_2O, 75.5 MHz): δ101.1, 80.8, 73.6, 71.3, 70.7, 67.5, 67.1, 61.8, 61.4, 57.8. ESI-MS *m/z*: calcd. for $C_{10}H_{20}O_8Na$: 291.1056; found: 291.1057 (M+Na). Anal. calcd. for $C_{10}H_{20}O_8$ +H_2O: C 41.95, H 7.69; found: C 41.35, H: 7.03.

2-Dodecyloxy-1,3-bis-O-(α-D-mannopyranosyl)-propane (5)

Yield: 60%, $[\alpha]_D^{24} = +54° = +54°$ (c=1.0, MeOH), ^{1}H NMR (300 MHz, DMSO-d_6): δ 4.71 (m, 4 H), 4.56 (m, 4 H), 4.44 (t, 2 H, J=4.5 Hz), 3.64–3.29 (band, 11 H), 1.43 (m, 2 H), 1.22 (br s, 18 H), 0.83 (t, 3 H, J=6.6 Hz). ^{13}C NMR (75.5 MHz, DMSO-d_6): 100.2, 76.8, 73.9, 70.9, 70.3, 69.5, 66.9, 66.3, 61.2, 31.3–22.1, 14.0. ESI-MS *m/z*: calcd. for $C_{27}H_{52}O_{13}Na$: 607.3306; found: 607.3280 (M+Na). Anal. calcd. for $C_{27}H_{52}O_{13}$+H_2O: C 53.82, H 8.64; found: C 53.37, H 9.01.

5-Dodecyloxy-1,9-bis-O-(α-D-mannopyranosyl)-3, 7-dioxanonane (6)

Yield: 63%, $[\alpha]_D^{24} = +45°$ (c=1.0, MeOH), ^{1}H NMR (300 MHz, DMSO-d_6): δ 4.73 (m, 4 H), 4.60 (m, 4 H), 4.45 (t, 2 H, J=6.0 Hz), 3.67–3.31 (band, 19 H), 1.43 (m, 2 H), 1.22 (br s, 18 H), 0.83 (t, 3 H, J=6.9 Hz). ^{13}C NMR (75.5 MHz, DMSO-d_6): δ99.9, 79.2, 77.2, 73.9, 70.9, 70.6, 70.3, 69.5, 66.9, 65.6, 61.2, 33.7–22.2, 14.0. ESI-MS *m/z*: calcd. for $C_{31}H_{60}O_{15}Na$: 695.3830; found: 695.3812 (M+Na). Anal. calcd. for $C_{31}H_{60}O_{15}$ + $2H_2O$: C 52.54, H 8.47; found: C 52.74, H 9.01.

8-Dodecyloxy-1,15-bis-O-(α-D-mannopyranosyl)-3,6,10, 13-tetraoxapentadecane (7)

Yield: 68%. $[\alpha]_D^{24} = +56°$ (c=1.0, MeOH). ^{1}H NMR (300 MHz, DMSO-d_6): δ4.62 (br s, 2 H), 3.65–3.42 (band, 35 H), 1.44 (m, 2 H), 1.24 (br s, 18 H), 0.83 (t, 3 H, J=6.6 Hz). ^{13}C NMR (DMSO-d_6, 75.5 MHz): δ99.9, 76.8, 73.9, 70.9, 70.6, 70.3, 69.8, 69.6, 69.4, 66.9, 66.2, 65.7, 61.3, 33.3–22.2, 14.0. ESI-MS *m/z*: calcd. for $C_{35}H_{68}O_{17}Na$: 783.4354; found: 783.4398 (M+Na). Anal. calcd. for $C_{35}H_{68}O_{17}$ + $3H_2O$: C 51.60, H 9.09; found: C 52.04, H 8.89.

2-Methoxy-1,3-bis-O-(α-D-mannopyranosyl)-propane (8)

Yield: 54%, $[\alpha]_D^{24} = +30°$ (c=1.0, MeOH), ^{1}H NMR (D_2O, 300 MHz): δ4.72 (br s, 2 H), 3.79 (m, 2 H), 3.73 (m, 2 H), 3.69 (m, 2 H), 3.59–3.53 (band, 4 H), 3.49–3.44 (band, 4 H), 3.28 (m, 3 H), 3.17 (s, 3 H) . ^{13}C NMR (D_2O, 75.5 MHz,): 101.4, 80.9, 71.3, 70.7, 67.5, 66.4, 61.7, 60.9, 57.7. ESI-MS *m/z*: calcd. for $C_{16}H_{30}O_{13}Na$: 453.1584; found: 453.1574 (M+Na). Anal. calcd. for $C_{16}H_{30}O_{13}$+$2H_2O$: C 41.20, H 7.29; found: C 40.47, H 6.93.

8-Dodecyloxy-3,6,10,13-tetraoxapentadecan-1,15-diol (NS)

^{1}H NMR (300 MHz, CD_3COCD_3): δ3.66–3.54 (band, 23 H), 1.55 (m, 2 H), 1.28 (br s, 18 H), 0.89 (t, J=6.6 Hz, 3 H). ^{13}C NMR (75.5, MHz, CD_3COCD_3): δ 78.8, 73.6, 71.8, 71.6, 71.1, 70.9, 61.8, 32.4–23.2, 14.0. HR-MS *m/z*: calcd. for $C_{23}H_{48}O_7Na$: 459.3298, found: 459.3267 (M+Na).

SPR experiments

The experiments were performed on a Biacore 2000 instrument, with research grade carboxymethylated dextran (CM5) sensor chip and Bioevaluation software (Biacore, Uppsala, Sweden).

Preparation of Con A surface on the CM5 sensor chip

After equilibration of the sensor surface with HEPES buffer (pH 7.4), the surface was activated at a flow rate of 20 μl/min with a 5 min pulse of 1:1 mixture of freshly prepared *N*-hydroxysuccinimide (NHS) (0.1 M) and *N*-ethyl-*N*′-(dimethyl-aminopropyl)carbodiimide (EDC) (0.1 M). Con A, at a concentration of 80 μg/ml in 10 mM NaOAc buffer (pH 4.3), was injected into channel 2. The remaining *N*-hydroxysuccinimide esters were blocked by the addition ethanolamine hydrochloride (1.0 M) at pH 8.5 for 3 min. Similarly, WGA was immobilized on channel 1 surface. After immobilization, the stability of the lectin immobilized surface was confirmed by three to four washes with regeneration solution (10 mM glycine–HCl, pH 2.5). The first wash with regeneration solution resulted in significant response decrease and the amount of loss in lectin surface decreased in the subsequent regeneration steps and the surface response stabilized after three washes. Approximately 5400 RU of Con A on Fc2 and 4900 RU of WGA on Fc1 were immobilized.

SPR kinetic experiments for the lectin–ligand interactions

All binding experiments with sugar ligands were performed at a flow rate of 20 μl/min using HEPES buffer (pH 7.4), as the eluant. Injection times of ligands were 105 s, followed by 105 s of dissociation phase. Regeneration was performed with 30 s pulse of glycine–HCl (pH 2.55). For the calculations of the kinetic constants, each sugar ligand was diluted in HEPES buffer, ranging from concentrations of 4, 8, 16, 32, 64 μM. Duplicate injections of each ligand were analysed in all kinetic experiments. The sugar ligands were diluted in the running buffer (HEPES, pH 7.4) to minimise the bulk effects. Each analyte solution was injected into channel 2 (Con A) and channel 1 (WGA). The specific response of the Con A surface towards the ligand was obtained by subtracting the channel 2 response from the channel 1 response. The kinetic sensorgrams were fitted to Langmuir 1:1 binding and the visual inspection of the plot of theoretical model *vs* experimental data provided that the χ^2 fitting agreed to the 1:1 Langmuir binding model. The mass transfer limitations were checked for the ligands and the mass transfer effects were found to be negligible.

ITC experiments

The experiments were performed using Microcal VP-ITC. In individual titrations, injection of 10 μl of sugar ligand were added from the computer controlled 300 μl microsyringe at an interval of 3 min into the Con A solution, dissolved in the same buffer as the ligand. The microsyringe was stirring at 300 rpm. All ITC experiments were

performed in HEPES buffer (10 mM) containing NaCl (150 mM), $CaCl_2$ (1 mM) and $MnCl_2$ (1 mM). The initial two injections were discarded from the data sheet in ordered to remove the effect of titrant diffusion across the syringe tip during the equilibration process. The experimental data were fitted to a one site binding model, with ΔH, K_a and n (no. of binding sites per monomer), as adjustable parameters. For all the experiments, the quantity, $c=K_aM_t(0)$, where $M_t(0)$ is the initial macromolecular concentration, was observed to be in the range of $4<c<20$. The concentration of Con A was determined spectrophotometrically at 280 nm using $A^{1\%}_{1\,cm} = 13.7$ at pH=7.4 and expressed in terms of the monomer (M_r=25,600) [26]. Control experiments were performed by making the identical injections of sugar ligands into a cell containing buffer with no protein.

Fluorometry

The critical micellar concentrations for each sugar ligand in buffer were measured using fluorometry [27]. Pyrene emission spectrum was obtained by exciting the sample at 332 nm and emission was recorded in the range of 360 to 460 nm. Different known concentrations of solutions were prepared with constant fluorescent probe concentration and the emission spectrum was recorded. The CMCs of each sugar ligand were determined at 25 °C.

Dynamic light scattering (DLS)

DLS experiments were performed on Brookhaven Instruments Ltd Systems, having a BI-200SM goniometer, a BI-APD digital correlator, a BI-APD photomultiplier and a Melles Griot He–Ne laser operated at 632.8 nm. The measurements were made at 20±1 °C and all the binding experiments were carried out in HEPES buffer (pH 7.4). The scattered light was collected at fixed angle of 90°. Prior to DLS experiments, protein or sugar ligand in buffer was individually filtered through inorganic membrane filters (Sartorius Minisart syringe filters, 0.2 μM) into separate vials. Each sample was filtered three to four times and then various portions of sugar ligand and protein were transferred into a sample cell for DLS measurements. The calculations of the particle size distribution averages were performed with ISDA software package, which employed single-exponential fitting, cumulants analysis and non-negatively constrained least-squares particle size distribution analysis routines.

Transmission electron microscopy (TEM)

Solutions of the complex (10 μl) (ligand: 50 μM; lectin : 8 μM, pH 7.4) were placed onto a carbon-coated copper grid and allowed to settle for 1–2 min and the remaining liquid was removed using a paper wick. Phosphotungastic acid (1%) (10 μl) solution was used to negatively stain the sample for 40 s. The samples were dried at room temperature for 2 h and the images were recorded on a JEOL 100 CX II TEM, at an acceleration voltage of 80 kV.

Results and discussion

The structures of the bivalent and monovalent glycolipid ligands studied are presented in Fig. 1. The linker lengths

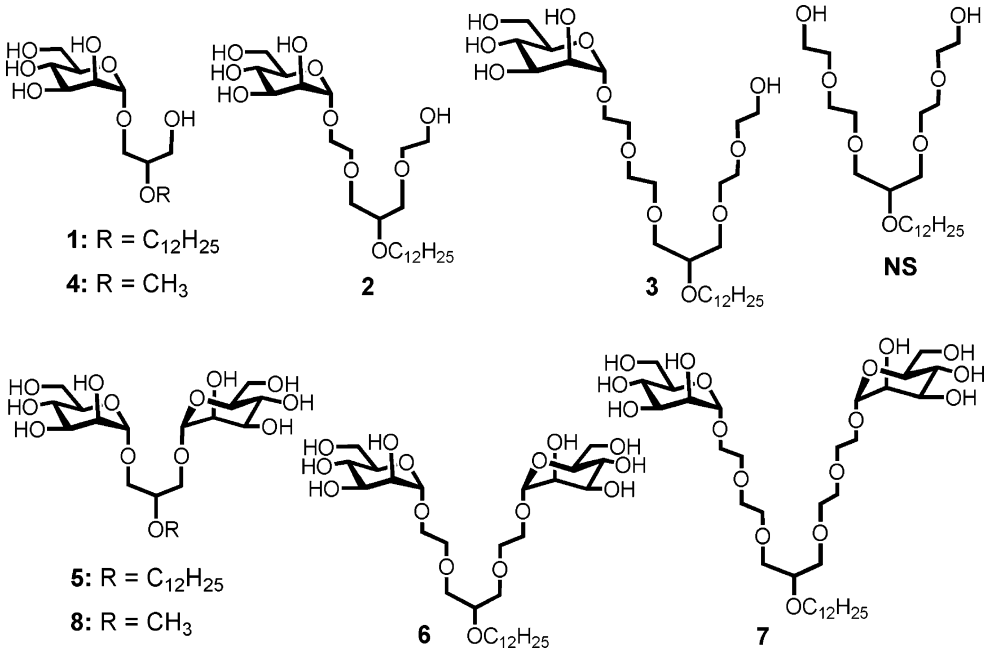

Fig. 1 Structures of mono- and bivalent sugar ligands *1–8* and non-sugar ligand *NS*

connecting the individual ligands in the bivalent structures were varied systematically by incorporation of the ethylene glycol units. In order to augment the amphiphilicities and glycolipidic nature in the ligands, a long alkyl chain was incorporated within the molecules. The monovalent structures with similar linker constitution were also prepared. Synthesis of the sugar ligands were performed through standard glycosylation protocols, involving the hydroxyl group protected glycosyl donors and hydroxyl group bearing aglycon acceptors. Thus, glycosylation of appropriate alcohols with one or two molar equivalents 2,3,4,6-tetra-*O*-benzoyl-α-D-mannopyranosyl bromide, followed by a deprotection protocol afforded the monovalent ligands *1–4* and the bivalent ligands *5–8*, respectively. A non-sugar ligand (*NS*) was also synthesized for comparison. The structural homogeneities of the ligands *1–8* and *NS* were confirmed by routine physical methods.

Due to the amphiphilic nature of the newly derived sugar ligands, their critical micellar concentrations (CMC) in aqueous solution were assessed. The aggregation studies were conducted by fluorescence method, using pyrene as the probe [27]. The CMCs were conducted in HEPES buffer. The following CMC was determined for each ligand. *1*: 0.20 mM; *2*: 0.14 mM; *3*: 0.09 mM; *5*: 0.43 mM; *6*: 0.29 mM; *7*: 0.24 mM. The general observations were that (1) the bivalent ligands *5* to *7* exhibited higher CMCs than the monovalent ligands *1* to *3* and (2) the ethylene glycol spacered ligands *2*, *3*, *6* and *7* presented lower CMCs than the ligands *1* and *5*, not having the spacer.

Assessment of the kinetic constants of the sugar ligand–lectin interactions by SPR

The series of bivalent and monovalent sugar ligands *1–8* were undertaken for lectin binding studies, addressing specifically the trends in the kinetic on–off rates that accompany the complexation. The SPR method is used widely for kinetic studies of biomolecular interactions, including carbohydrate–protein interactions [28–32]. In the present study, the sugar ligands *1–8* were used as analytes on the lectin coated carboxymethylated dextran sensor surface. The choice of the lectin immobilized surface was to enable the screening of a number of analytes on the same surface, which was regenerated after experiments with each analyte. Thus, a surface immobilization with lectin Con A was generated. As a control, lectin WGA immobilized surface was also undertaken for the studies, as WGA does not recognize α-D-mannopyranosides [33]. The protocol involved immobilization of the lectin on the CM5 surface through an amidation of the carboxylic acid moieties of the surface with amine moieties of the lectin, mediated by the amine coupling reagents NHS and EDC. The response unit of immobilization was approximately 5400 RU for the lectin Con A and 4900 RU for the lectin WGA. These lectin surfaces were maintained as separate flow cells and the sugar ligands acted as the analytes. The concentrations of the ligands were maintained below their respective CMCs, so as to allow the interactions of monomeric ligands with the lectin binding sites. The relative response units corresponding to the association phase and the subsequent equilibrium and dissociation phases were measured as a function of the response difference between Con A and WGA surfaces. Figure 2 shows the sensorgrams obtained for the interactions of mono- and bivalent ligands with the lectin. As anticipated, a significant increase in the response units were observed for the ligand–Con A interactions. The low response units referred primarily to the interactions of the monomeric ligands with the lectin. All the ligands were allowed association/equilibrium phases for 105 s and following these phases, the decomplexation, *i.e.* the dissociation phase, was initiated by passing the buffer alone over the surface and continued for 105 s. Upon decomplexation, the surfaces were regenerated by using a 30 s pulse of glycine–HCl (pH 2.5). The non-sugar ligand NS did not exhibit any response unit. Further, low molecular weight ligands 4 and 8, not possessing the alkyl chains within the ligand, did not exhibit a detectable response unit over the Con A surface. From these ligand–lectin interaction sensorgrams, the following observations were made: (1) within the mono-

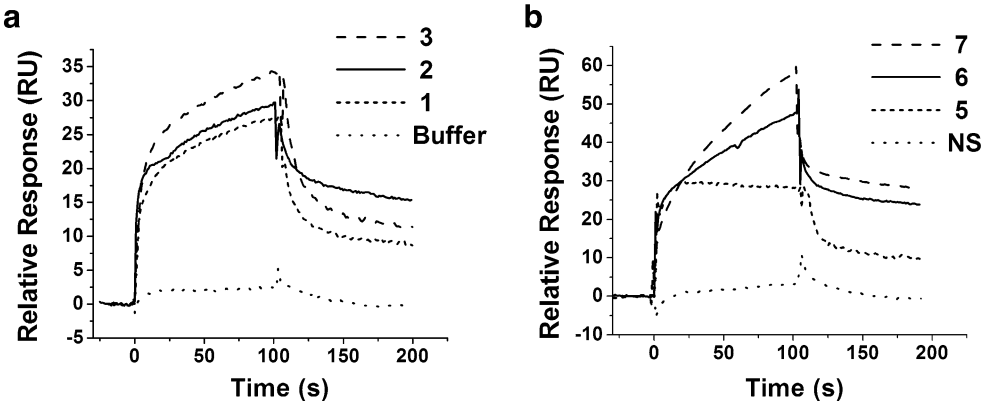

Fig. 2 The relative responses obtained for the binding of **a** monovalent sugar ligands and **b** bivalent sugar ligands to the immobilized lectin, at a ligand concentration of 64 μM

and bivalent series, the response units increased in the series *1–3*, and *5–7*; (2) the equilibrium responses were attained within 105 s in the monovalent series; (3) the association response gradually increased for the bivalent ligands *6* and *7* and reached a saturation after 3 min. Subsequently, the bivalent ligands *6* and *7* exhibited higher response units, in comparison to the monovalent ligands [34].

The kinetic studies of the ligand–receptor interactions were carried out by conducting the experiment at varied concentrations. Figure 3a shows the sensorgrams obtained for the interaction of *6* with Con A. The solid lines in the figure represent the observed sensorgrams and the dotted lines represent the global fit of the data on a 1:1 Langmuir binding model. To assess the mass transfer limitation, a fixed concentration of the ligand *6* (64 μM) was passed over the Con A surface at different flow rates 5, 15 and 75 μl/min. The sensorgrams thus obtained did not differ, thereby excluded the possibility of mass transfer limitation (Fig. 3b).

Table 1 summarizes the analysis of the ligand–Con A interactions. The analyses were guided by χ^2 value which refers to the best fit of the theoretical model *vs* the experimental data. A Langmuir 1:1 binding model agreed well with the observed χ^2 values. It was observed that the bivalent ligands *6* and *7* exhibited relatively faster association (k_a) and slower dissociation (k_d) rate constants, than the remaining ligands. Interestingly, the bivalent ligand *5*–lectin interactions had provided only a marginal increase in the k_a value, when compared to the monovalent ligands. The most important outcome of the SPR studies is the identification that the k_a and k_d, relating to the association and dissociation rate constants, respectively, are distinctly different to the bivalent ligands, in comparison to the monovalent ligands. Specifically, the k_a increased, whereas the k_d decreased for the bivalent ligand–lectin interactions. The bivalent ligand with longer spacers, namely, ligand *7* showed higher k_a than ligand *6*. While an increase in binding constants (K_a) is seen most commonly due to multivalent interactions, the SPR studies herein show, for the first time, that the kinetic rate constants also differ significantly in the bivalent sugar ligand–lectin interactions.

Table 1 Kinetic parameters for sugar ligand–Con A interactions at 25 °C

Ligand	k_a ($M^{-1}s^{-1}$)	K_d (s^{-1})	χ^2
1	1.43×10^2	9.45×10^{-3}	3.1
2	1.38×10^2	5.42×10^{-3}	2.0
3	$1.\ 26\times10^2$	7.77×10^{-3}	3.4
5	1.61×10^2	4.19×10^{-3}	3.8
6	1.96×10^2	1.67×10^{-3}	0.6
7	4.77×10^2	2.18×10^{-3}	1.5

Study of the sugar ligand–Con A interactions by ITC

In order to correlate the functional valencies in the bivalent ligands *5–7* and to assess the thermodynamic parameters, ITC studies were undertaken. The studies were conducted at a ligand concentration much below their CMCs and in HEPES buffer (pH 7.4). Figure 4 shows the thermograms obtained for the complexation of ligand *2* or *6* with Con A.

Results of the ITC studies are summarized in Table 2. It was found that the stoichiometry (*n*) of lectin binding by each ligand was close to 1, whereas the bivalent ligands *6* and *7* showed an *n* value of 0.5. The bivalent ligand *5*, without an ethylene glycol spacer, presented an *n* value of ~1.0. The bivalent ligands *6* and *7* exhibited logarithmic enhancements in the binding affinities, while the monovalent ligand had also shown several fold enhancement in comparison to Me-α-Man. The presence of the long alkyl chain influenced increases in the binding constants, as can be seen by comparing ligands *1*, *4* and Me-α-Man. The enhancement in the binding affinities in the monovalent ligands *1–3* and the bivalent ligand *5* can thus be attributed to the presence of hydrophobic interactions, as evidenced by the positive entropy changes. On the other hand, logarithmic enhancement in the binding constants for the bivalent ligands *6* and *7* were due to favourable enthalpy

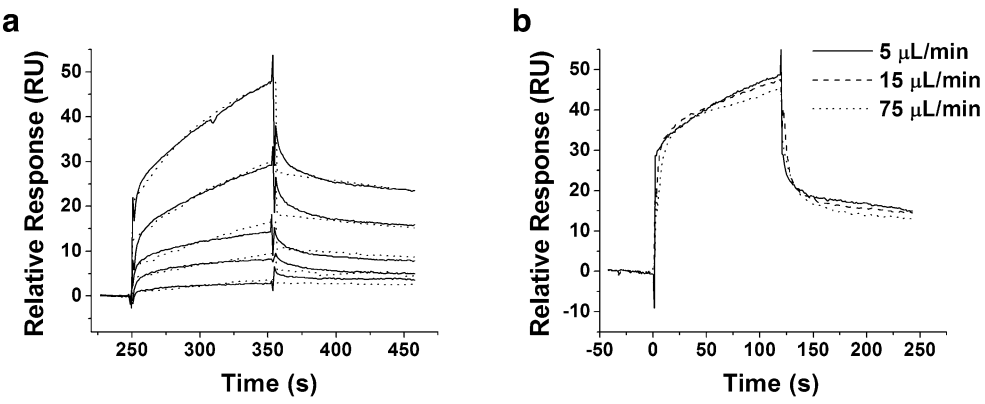

Fig. 3 **a** SPR sensorgrams of the kinetics of *6* and Con A interactions at a concentrations of 4, 8, 16, 32 and 64 μM (*bottom to top*). *Solid lines* represent experimental data and *dotted lines* represent the Langmuir binding (1:1) analysis fit. **b** Sensorgrams obtained for the binding of *6* to Con A in a mass transfer control experiment

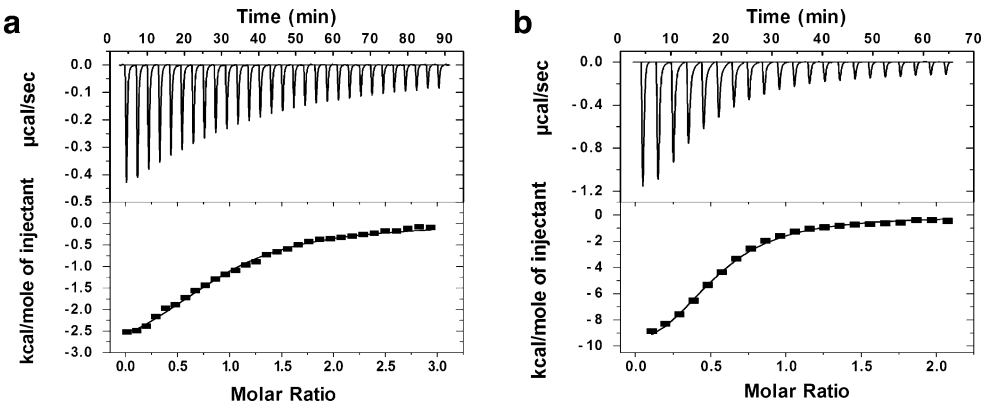

Fig. 4 ITC raw and integrated data for **a** *2*-Con A and, **b** *6*-Con A interactions. The experimental points represented as *filled squares* and the best fit of these points with one site binding model is represented as *solid curve*

changes and cross-linking of the lectin by the ligands. The cross-linked complex formation could be observed by visible precipitation of the complex from the solution, upon saturation of the binding sites. A query was then looked into as to the probable formation of cross-linked complexes that prevail in the solution phase. The query was addressed by assessing the nature of the ligand–lectin complex by DLS and by TEM.

Characterization of the ligand–lectin complexes by DLS and TEM

For the DLS studies, the ligand concentrations were maintained very low due to the sensitivities of the method. The measurement provides the hydrodynamic diameter and uniformities in the sizes of the particles [35]. The DLS measurement of the Con A alone showed a hydrodynamic diameter centered at 8 nm. This observed diameter agreed well with the value reported previously for the lectin [36]. Representative DLS plots of Con A and its complexes with ligands *5*–*7* are presented in Fig. 5. The functionally monovalent ligand *5*-lectin complex presented a hydrodynamic diameter at ~8 nm, resembling that of the lectin alone. However, it was noticed that the width of distribution histogram, which denoted the spread of the particle size, was narrower for the *5*-lectin complex, than the lectin alone. Qualitatively, this suggests a possible reduction in the overall diameter of the lectin, upon ligand binding.

Table 2 Binding stoichiometries and thermodynamic parameters of sugar ligand–Con A interactions at 25 °C

Ligand	N	K_a ($\times 10^{-4}$)	ΔG	ΔH	$T\Delta S$
1	0.91	9.14 (±0.75)	−6.76	−3.39	3.37
2	1.01	5.76 (±0.80)	−6.49	−3.98	2.51
3	1.09	7.06 (±1.23)	−6.61	−3.01	3.60
4	1.03	0.86 (±0.06)	−5.36	−7.9	−2.62
5	1.10	5.75 (±0.27)	−6.49	−6.39	0.10
6	0.50	20.6 (±1.7)	−7.59	−12.80	−5.21
7	0.47	37.4 (±2.4)	−7.61	−11.54	−3.93
8	1.05	2.48 (±0.12)	−5.99	−6.3	−0.32
*Me*αMan	1.04	0.79 (±0.04)	−5.27	−7.83	−2.56

K_a is in the unit of M^{-1}; ΔG, ΔH and $T\Delta S$ are in the units of kcal mol^{-1}. Errors in ΔG are ~1–4%. Errors in ΔH are in the range of 1–8%. Errors in $T\Delta S$ are in the range of 1–6%.

The ligand–lectin complexes corresponding to bivalent ligands *6* and *7* led to the identification of larger aggregate sizes. Whereas higher amounts of very large particle sizes were observed for the *7*-lectin complexes, an intense population of *6*-lectin complex with a hydrodynamic diameter centering at 16 nm was observed. This value corresponds to the sum of two lectin tetramers that are brought together upon binding by the bivalent ligand *6*. Thus, an onset of intermolecular cross-linked complex formation could be identified through an increase in the diameter of the complex. In addition to the dimeric complexes, a small population of larger aggregates could also be seen in the histogram of *6*-lectin complex. It is clear that the cross-linking of the lectin by the ligands is initiated from the early stages of the binding process and that the cross-linked complex acts as initiation points for larger aggregates to form, as a function of further ligand binding. While the cross-linked complexes were identified previously as a result of visible precipitation of the complex from the solution [19], the DLS study herein shows, the presence of intermolecular cross-linked complex, which exists in solution from the initial stages of the ligand–lectin binding process. Polydispersity values of the hydrodynamic diameter were in the range of 14–23% in all the histograms and this range indicated fairly uniform sizes of the oligomeric complexes. From the DLS studies, it appears that it is possible to generate well-defined oligomeric species of lectin through cross-linking mediated by the designed ligands.

Upon realizing the diameter of the ligand–lectin complexes by DLS, an attempt was undertaken to visualize the complexes by TEM. Solutions of fixed molar ratios of the ligand and the lectin were prepared and the solutions were cast onto the copper-coated carbon grid. After drying, the samples were negatively stained with phosphotungastic acid and dried further. The TEM images thus obtained for

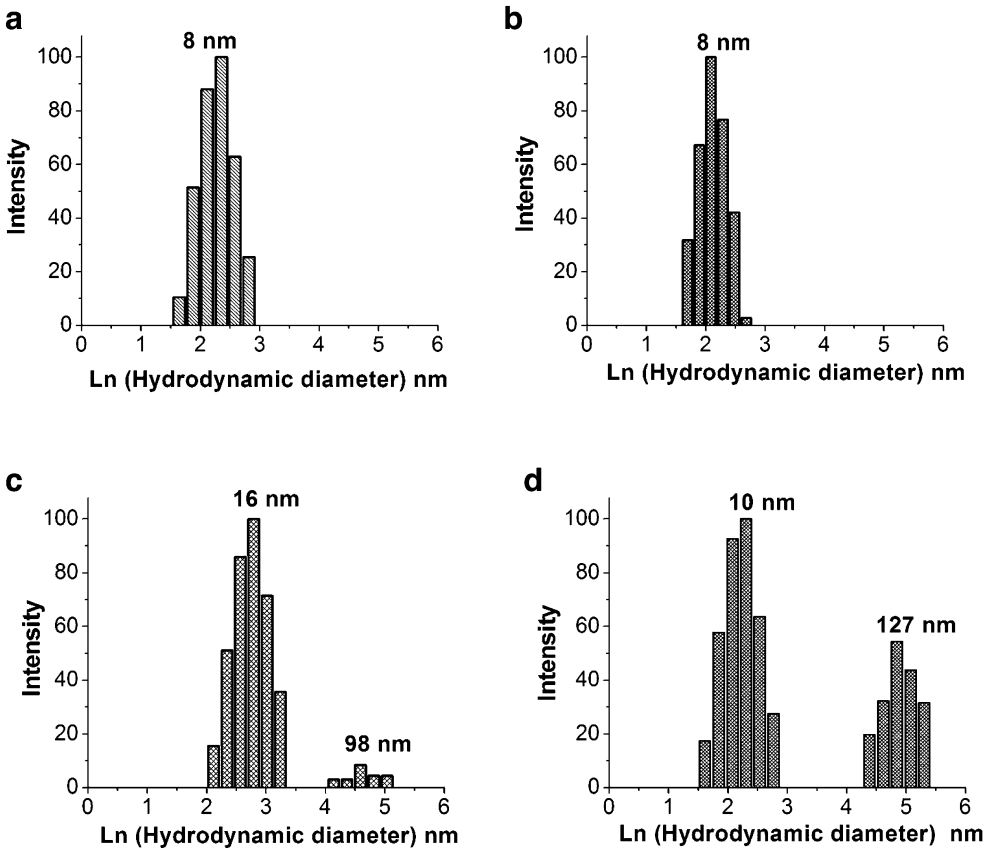

Fig. 5 Hydrodynamic diameter distribution of: **a** Con A; **b** *5* + Con A; **c** *6* + Con A and **d** *7* + Con A complexes

the bivalent ligands *5* to *7*-lectin complexes are presented in Fig. 6. The complex 5–Con A exhibited particle sizes in the range of 5–10 nm, matching nearly the size of the lectin alone. On the other hand, *6*-Con A and *7*-Con A complexes provided sizes varying between 40–150 nm. These particle sizes corresponded to similar aggregate sizes derived from the DLS studies. The TEM studies thus complement directly the solution phase observations made through the DLS measurements.

In conclusion, the study described herein provides a detailed insight into the kinetics of the modest bivalent ligand–lectin interactions, in comparison to the monovalent ligands. The rate constants for the ligand–lectin associations are significantly higher for the bivalent ligands, than for the monovalent ligands. This increase in k_a relates to an intermolecular binding process, in the present study. The kinetic studies of ligand–lectin interactions, in general, are not known in detail presently. The kinetic studies presented herein are thus valuable and important in the mechanistic queries of the ligand–lectin complexations. The kinetic studies are combined with studies of the thermodynamics of the ligand–lectin interactions. In addition to evaluating the kinetic and thermodynamic parameters, the results also allowed estimation of the influence of the hydrophobicities and functional bivalencies. The DLS and TEM characterizations further show the status of the complexation with differing ligand constitutions and the oligomeric complex sizes and the morphologies. The results obtained in this study should be useful in ligand design for effective ligand–lectin interactions.

Acknowledgement We thank Department of Science and Technology, New Delhi, for a financial support. We thank Professor Venugopal and Mr. Alok for DLS measurements. BNM thanks the Council of Scientific and Industrial Research for a research fellowship.

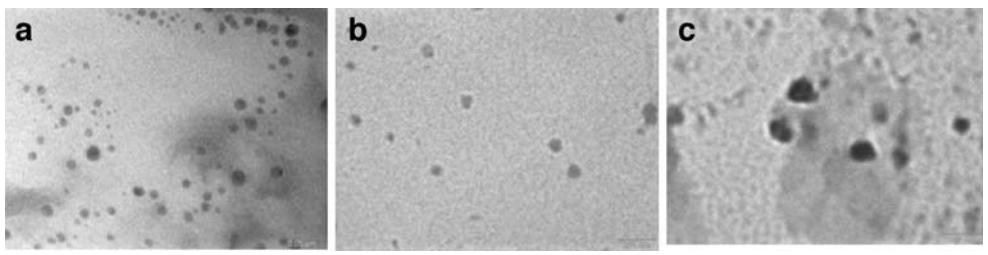

Fig. 6 TEM images of ligand–lectin complexes: **a** *5*-Con A; **b** *6*-Con A and **c** *7*-ConA. Scale bar: **a** 50 nm; **b** 200 nm and **c** 200 nm

References

1. Sharon, N., Lis, H.: Lectins as cell recognition molecules. Science **246**, 227–234 (1989)
2. Lee, Y.C., Lee, R.T.: Carbohydrate–protein interactions: basics of glycobiology. Acc. Chem. Res. **28**, 321–327 (1995)
3. Wong, C.-H.: Carbohydrate-based Drug Discovery, 1st edn. (vols 1 and 2). Wiley-VCH, Weinheim, (2003)
4. Dwek, R.A.: Glycobiology: toward understanding the function of sugars. Chem. Rev. **96**, 683–720 (1996)
5. Crocker, P.R., Feizi, T.: Carbohydrate recognition systems: functional triads in cell–cell interactions. Curr. Opin. Struct. Biol. **6,** 679–691 (1996)
6. Dam, T.K., Brewer, C.F.: Thermodynamic studies of lectin–carbohydrate interactions by isothermal titration calorimetry. Chem. Rev. **102**, 387–430 (2002)
7. Lundquist, J.J., Toone, E.J.: The cluster glycoside effect. Chem. Rev. **102**, 555–578 (2002)
8. Mammen, M., Choi, S.-K., Whitesides, G.M.: Polyvalent interactions in biological systems: implications for design and use of multivalent ligands and inhibitors. Angew. Chem. Int. Ed. **37**, 2754–2794 (1998)
9. Monsigny, M., Mayer, R., Roche, A.C.: Sugar–lectin interactions: sugar clusters, lectin multivalency and avidity. Carbohydr. Lett. **4**, 35–52 (2000)
10. Kiessling, L.L., Gestwicki, J.E., Strong, L.E.: Synthetic multivalent ligands as probes of signal transduction. Angew. Chem. Int. Ed. **45**, 2348–2368 (2006)
11. Fan, E., Zhang, Z., Minke, W.E., Hou, Z., Verlinde, C.L.M.J., Hol, W.G.J.: High-affinity pentavalent ligands of *Escherichia coli* heat-labile enterotoxin by modular structure-based design. J. Am. Chem. Soc. **122**, 2663–2664 (2000)
12. Pavel, I.K., Joanna, M.S., George, M., Glen, D.A., Hong, L., Navraj, S.P., Randy J.R., Bundle, D.R.: Shiga-like toxins are neutralized by tailored multivalent carbohydrate ligands. Nature **403**, 669–672 (2000)
13. Turnbull, W.B., Kalovidouris, S.A., Stoddart, J.F.: Synthetic carbohydrate dendrimers. Part 9. Large oligosaccharide-based glycodendrimers. Chem. Eur. J. **8**, 2988–3000 (2002)
14. Roy, R.: Syntheses and some applications of chemically defined multivalent glycoconjugates. Curr. Opin. Struct. Biol. **6**, 692–702 (1996)
15. Reina, J.J., Maldonado, O.S., Tabarani, G., Fieschi, F., Rojo, J.: Mannose glycoconjugates functionalized at positions 1 and 6. Binding analysis to DC-SIGN using biosensors. Bioconjug. Chem. **18**, 963–969 (2007)
16. Reiger, J., Stoffelbach, F., Cui, D., Imberty, A., Lameignere, E., Jerome, C., Amely-velty, R.: Mannosylated poly(ethylene oxide)-b-Poly(ε-caprolactone)diblock copolymers: synthesis, characterization, and interaction with a bacterial lectin. Biomacromolecules **8**, 2717–2725 (2007)
17. Mangold, S.L., Cloninger, M.J.: Binding of monomeric and dimeric Concanavalin A to mannose-functionalized dendrimers. Org. Biomol. Chem. **4**, 2458–2465 (2006)
18. Gestwicki, J.E., Cairo, C.W., Strong, L.E., Oetjen, K.A., Kiessling, L.L.: Influencing receptor–ligand binding mechanisms with multivalent ligand architecture. J. Am. Chem. Soc. **124**, 14922–14933 (2002)
19. Dam, T.K., Oscarson, S., Roy, R., Das, S.K., Page, D., Macaluso, F., Brewer, C.F.:Thermodynamic, kinetic, and electron microscopy studies of concanavalin A and Dioclea grandiflora lectin cross-linked with synthetic divalent carbohydrates. J. Biol. Chem. **280**, 8640–8646 (2005)
20. Srinivas, O., Mitra, N., Surolia, A., Jayaraman, N.: Photoswitchable multivalent sugar ligands: synthesis, isomerization and lectin binding studies of azobenzene–glycopyranoside conjugates. J. Am. Chem. Soc. **124**, 2124–2125 (2002)
21. Srinivas, O., Mitra, N., Surolia, A., Jayaraman, N.: Photoswitchable cluster glycosides as tool to probe carbohydrate–protein interactions: synthesis and lectin-binding studies of azobenzene containing multivalent ligands. Glycobiology **15**, 861–873 (2005)
22. Murthy, B.N., Sampath, S., Jayaraman, N.: Synthesis and Langmuir studies of bivalent and monovalent α-D-mannopyranosides with Lectin Con A. Langmuir **21**, 9591–9596 (2005)
23. Murthy, B.N., Voelcker, N.H., Jayaraman, N.: Evaluation of α-D-mannopyranoside glycolipids–lectin interactions by surface plasmon resonance methods. Glycobiology **16**, 822–832 (2006)
24. Cassel, S., Debig, C., Benvegnu, T., Chaimbault, P., Lafosse, M., Plusquellec, D., Rollin, P.: Original synthesis of linear, branched and cyclic oligoglycerol standards. Eur. J. Org. Chem. **2001**, 875–896 (2001)
25. Ness, R.K., Fletcher, Jr H.G., Hudson, C.S.: The reaction of 2,3,4,6-tetrabenzoyl-α-D-glucopyranosyl bromide and 2,3,4,6-tetrabenzoyl-α-D-mannopyranosyl bromide with methanol. Certain benzoylated derivatives of D-Glucose and D-Mannose. J. Am. Chem. Soc. **72**, 2200–2205 (1950)
26. Goldstein, I.J., Poretz, R.D.: The Lectins: Properties, Functions and Applications in Biology and Medicine. Academic, New York, pp. 35–244 (1998)
27. Goddard, E.D., Turro, N.J., Kuo, P.L.: Ananthapadmanabhan KP, Fluorescence probes for critical micelle concentration determination. Langmuir **1**, 352–355 (1985)
28. Monsigny, M., Frison, N., Duverger, E., Roche, C.A.: Carbohydrate–protein interactions assessed by surface plasmon resonance. Biochemie **85**, 167–179 (2003)
29. Surolia, A., Sharma, S., Sikder, B.K., Thomas, J.C., Kapoor, M.: Exploring kinetics and mechanism of protein–sugar recognition by surface plasmon resonance. Methods Enzymol. **362**, 312–329 (2003)
30. Gallego, R.E., Haseley, H.R., van Miegem, V.F.L., Vliegenthart, J. F.G., Kamerling, J.P.: Identification of carbohydrates binding to lectins by using surface plasmon resonance in combination with HPLC profiling. Glycobiology **14**, 373–386 (2004)
31. Kisseling, L.L., Maly, J.D., Kanai, M., Mann, A.D.: Probing low affinity and multivalent interactions with surface plasmon resonance: ligands for Concanavalin A. J. Am. Chem Soc. **120**, 10575–10582 (1998)
32. Myszka, D.G., Hansely, P., Simons, S.P., Lemotte, P.K., Brown, T. A., Geoghegan K.F., Hoth, L.S., Rich, R.L.B.: Kinetic analysis of estrogen receptor/ligand interactions. Proc. Natl. Acad. Sci. USA **99**, 8562–8567 (2002)
33. Nagata, Y., Burger, M.M.: Wheat germ agglutinin: molecular characteristics and specificity for sugar binding. J. Biol. Chem. **249**, 3116–3122 (1973)
34. An alternate protocol of the ligand immobilization onto the sensor surface was attempted. Thus, ligand *7* was self-assembled into an alkyl thiol functionalized HPA surface. The lectin was introduced as the analyte and an increase in the SPR response, corresponding to the lectin binding onto the ligand-immobilized surface, was observed. However, the subsequent dissociation phase and the regeneration of the sensor surface devoid of the lectin led to drastic decreases in the response units, denoting the loss of the ligand also from the surface during the dissociation and surface regeneration steps. In the light of the loss of the immobilized ligand after the de-complexation, this alternate effort could not be continued further
35. Berne, B.J., Pecora, R.: Dynamic Light Scattering. Wiley, New York (1976)
36. Parkin, S., Rupp, B., Hope, H.: Atomic resolution structure of Con A at 120 K, Acta Cryst **D52**, 1161–1168 (1996)